Optical Absorptivity versus Molecular Composition of Model Organic Aerosol Matter

Angela G. Rincón,[†] Marcelo I. Guzmán,[‡] M. R. Hoffmann,[†] and A. J. Colussi*,[†]

W. M. Keck Laboratories, California Institute of Technology, Pasadena, California 91125, School of Engineering and Applied Sciences and Department of Earth and Planetary Sciences, Harvard University, Cambridge, Massachusetts, 02138

Aerosol particles affect the Earth's energy balance by absorbing and scattering radiation according to their chemical composition, size, and shape. It is generally believed that their optical properties could be deduced from the molecular composition of the complex organic matter contained in these particles, a goal pursued by many groups via high-resolution mass spectrometry, although: (1) absorptivity is associated with structural chromophores rather than with molecular formulas, (2) compositional space is a small projection of structural space, and (3) mixtures of polar polyfunctional species usually exhibit supramolecular interactions. Here we report a suite of experiments showing that the photolysis of aqueous pyruvic acid (a proxy for aerosol α-dicarbonyls absorbing at $\lambda > 300$ nm) generates mixtures of identifiable aliphatic polyfunctional oligomers that develop absorptions in the visible upon standing in the dark. These absorptions and their induced fluorescence emissions can be repeatedly bleached and retrieved without carbon loss or ostensible changes in the electrospray mass spectra of the corresponding mixtures and display unambiguous signatures of supramolecular effects. The nonlinear additivity of the properties of the components of these mixtures supports the notion that full structural speciation is insufficient and possibly unnecessary for understanding the optical properties of aerosol particles and their responses to changing ambient conditions.

Introduction

Unraveling the physical basis of climate change has become a pressing matter.[1,2] Among the various natural and anthropogenic factors driving this change, the role of atmospheric aerosols is least understood.[3–5] Aerosol particles (APs) affect the Earth's energy balance directly by absorbing and scattering radiation[6,7] and indirectly by altering the reflectance and persistence of clouds.[8–12] Direct effects depend on AP absorption coefficient $\sigma(\lambda)$ and single scattering albedo ω_0,[13] whereas indirect effects stem from their ability to nucleate water vapor.[14,15] Current fourth-generation climate models[16] generally assume that aerosols are composites of chemically different particles rather than particles consisting of homogeneous mixtures.[17] Invoking external mixing reduces the computational cost of parametrizing AP optical properties and their dependence on meteorological variables such as relative humidity (RH)[18–22] but may be unrealistic. This is a key issue because more than half of AP mass usually consists of an internal mixture of water-soluble complex organic matter (OM).[23–29] Uncertainties in the radiation budget of the troposphere are dominated by our inability to model AP forcings, particularly those due to OM.[1,16,30–35]

A more realistic representation of the optical properties of aerosol OM[30,36–38] is one of the top priorities of later generation climate models.[16] The implicit premise guiding ongoing efforts is that $\sigma(\lambda)$ is uniquely determined by the chemical constituents of OM.[39–41] This seemingly unassailable approach is being pursued by two presumably convergent methodologies that involve comprehensive chemical analysis, largely via ultra-high-resolution mass spectrometry (HR-MS) of natural OM,[39] and the OM produced in

smog-chambers.[42] Mass spectra of these materials resemble those of natural humic substances (hence their alternative designation as humic-like substances, HULIS)[40] displaying a daunting variety of $C_xH_yO_z$ species in the 100−1500 Da range, most of which have not been structurally characterized.[41,43–47]

This reductionist approach to the optical properties of AP faces two essential limitations.[48] First, because $\sigma(\lambda)$ is associated with chromophores and their couplings rather than with molecular formulas, the compositional space provided by HR-MS is only a small subset of the structural space that would be required to synthesize the optical properties of OM.[49] The number of constitutional $C_xH_yO_z$ isomers increases exponentially with mass, reaching $\sim 10^4$ at ~ 500 Da.[49] It is now realized that complex nonrepetitive systems, such as natural OM, can be operationally defined only by their properties rather than in terms of their intrinsically elusive chemical structures.[50–52] Second, and perhaps more crucially, even if complete structural speciation were achieved, the optical properties of mixtures of polar, polyfunctional molecules $\sigma(\lambda)$ should not be expected, in general, to be linear superpositions of the optical properties of individual components $\sigma_i(\lambda)$, that is, $\sigma(\lambda) \neq \Sigma x_i \sigma_i(\lambda)$. Supramolecular noncovalent interactions of various types (hydrogen bonding, charge transfer, van der Waals, etc.) between polyfunctional chromophores are the norm rather than the exception.[48,53–64] It has been pointed out, after more than a century of research, that humic substances are best described as supramolecular associations of low-molecular-mass organic molecules and that their characterization should focus on properties arising from intermolecular interactions rather than on molecular composition.[48,53]

The nonadditivity of optical properties thus renders full speciation an insufficient basis for characterizing OM's $\sigma(\lambda)$ or its dependences on RH, temperature, or insolation.[65] It is neither necessary because extreme chemical complexity ultimately

* Corresponding author. E-mail: ajcoluss@caltech.edu.
† California Institute of Technology.
‡ Harvard University.

Optical Absorptivity versus Molecular Composition

J. Phys. Chem. A, Vol. 113, No. 39, 2009 **10513**

implies that the same macrostates (e.g., optical properties) can be realized by a myriad of microstates (i.e., molecular formulas).[66] The sheer molecular complexity of OM, which accommodates almost any conceivable $C_xH_yO_z$ formula in the <1500 Da range,[67,68] makes their mass spectra virtually indistinguishable from those of other complex materials likely having dissimilar optical properties. This circumstance opens up the possibility of gaining insight into the origin of OM optical properties from simpler model mixtures.[23,69–73]

Herein we report kinetic, optical absorption, fluorescence,[74–82] and total organic carbon (TOC) measurements in a model system of tractable chemical complexity,[83] as monitored by direct infusion electrospray ionization mass spectrometry (ESI-MS). The objective of this article is to demonstrate the reality and environmental implications of the above phenomena by tracking the optical and chemical transformations of a simplified system subjected to the photochemical and thermal cycles experienced by atmospheric aerosols. Accordingly, this article does not attempt to reproduce the absorptivity of natural OM, partially because OM designates a class of related materials rather than a standard specimen and because other experimental variables, not considered herein, may significantly influence absolute $\sigma(\lambda)$ values.[84] The evidence of supramolecular interactions provided by these experiments should preclude assigning observations to specific molecular structures. Remarkably, we find that molecular complexity is preserved even under intense insolation; that is, organic photochemistry in concentrated aqueous aerosol phases involves both molecular degradation and aggregation processes.[85–88]

Experimental Section

Aqueous pyruvic acid (PA, Aldrich 98% bidistilled at reduced pressure) solutions (3.5 mL) were photolyzed (typically for 4.5 h, under continuous air sparging, at 293 K) in silica cuvettes (1 cm optical path length) with light from a 1 kW high-pressure Xe–Hg lamp filtered through water (to remove infrared radiation) and a 305 nm long-pass filter (Oriel). Photolyzed solutions were analyzed immediately or subsequently aged in the dark in closed cuvettes maintained at constant temperature for variable periods. Some aged solutions were rephotolyzed while being sparged with air and otherwise reprocessed over similar cycles. UV–visible absorption spectra were recorded with a spectrophotometer (Agilent 8453) provided with a temperature-controlled cuvette holder (HP-89090A). Negative ion mass spectra of directly infused sample solutions (previously diluted with chromatographic grade methanol, Chromasolv, purity >99.9%) were acquired using a ±0.1 Da resolution electrospray ionization mass spectrometer (Agilent 1100). TOC was determined with a TOC analyzer (Aurora 1030) calibrated with a potassium phthalate standard solution. Corrected excitation fluorescence spectra (i.e., directly comparable with UV absorption spectra) and uncorrected emission spectra were recorded in a luminescence spectrometer (Perkin-Elmer LS 50B) at 293 K, from which water Raman peaks were subtracted from all spectra using Milli-Q water as blank.

Results

Figure 1A shows UV–vis absorption spectra of 80 mM aqueous PA solutions before photolysis and after each of the following successive steps: (1) photolysis for 4.5 h under continuous air sparging, (2) thermal aging in the dark at 298 K for 15 h, or (3) thermal aging in the dark at 333 K for 72 h in closed cuvettes, and (4) 1:2 dilution of the mixture after step 3. (See Scheme S1 in the Supporting Information.) We recently
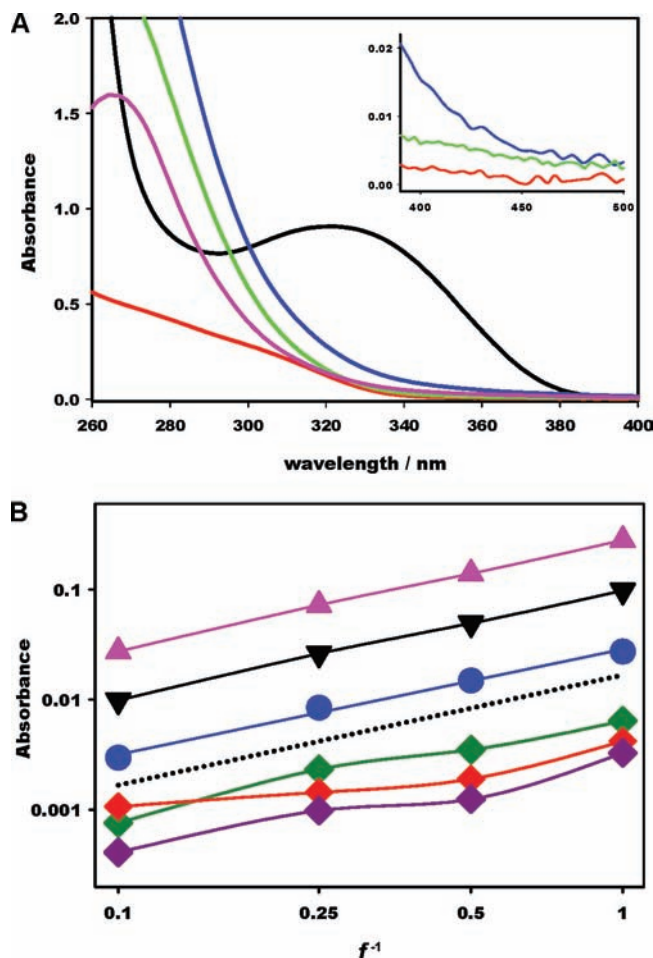

Figure 1. (A) UV–vis spectra. Black line: the initial 80 mM pyruvic acid (PA) solution. Red line: after 4.5 h photolysis. Green line: after 4.5 h photolysis, followed by 15 h in the dark at 298 K. Blue line: after 4.5 h photolysis, followed by 3 days in the dark at 333 K. Pink line: the previous solution diluted 1:2. (B) Absorbances of 80 mM PA solutions after 4.5 h photolysis, followed by thermal treatment at 333 K versus (dilution factor)$^{-1}$ at λ(nm) = 320 (▲, pink), 340 (▼, black), 380 (●, blue), 440 (◆, green), 490 (◆, red), 500 (◆, purple).

found that the relatively weak visible absorptions that arise in this system are greatly magnified by the addition of inert electrolytes.[84] Figure 1B is a log–log plot that shows how absorbances $A(\lambda)$ after step 3 decrease upon successive $1/f$ dilutions with water. It is apparent that Beer's law (the dashed line) is closely followed up to $\lambda \lesssim 350$ nm but not at longer wavelengths. This finding bears on current schemes for estimating $\sigma(\lambda)$ of APs as functions of RH on the basis of the linear additivity of the volume fractions of their components.[16]

Figure 2A shows how photolyzed mixtures held at 298 K (step 2 above) develop absorptions across the spectrum as a function of time.[89–91] Absorbances $A(\lambda)$ increase as single-exponential growth functions only at the shortest wavelengths. This behavior, however, does not extend to the near-ultraviolet and visible regions: the moieties absorbing at longer wavelengths are produced with complex kinetics at increasingly slower rates.[89] Figure 2B shows the faster kinetics of color development upon thermal treatment at 333 K before and after a 1:2 dilution with water, which implicate a process having sizable activation energy.

Figure 3A shows uncorrected fluorescence emission spectra of the solutions obtained after step 3 at excitation wavelengths spanning the range $290 \leq \lambda_{exc}/nm \leq 470$. It is apparent that emission spectra remain bounded by a long-wavelength
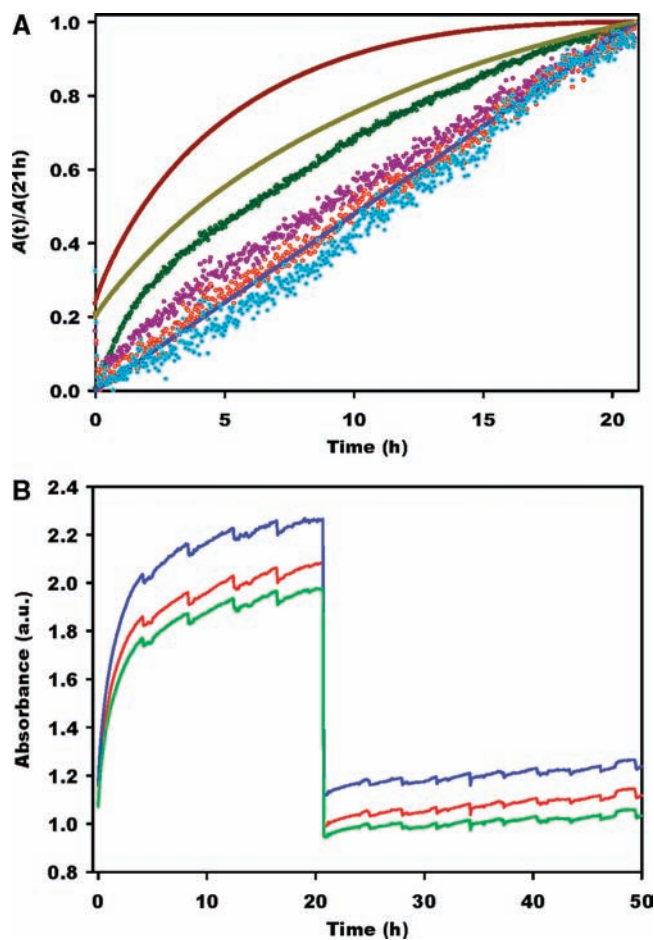
Figure 2. (A) Normalized absorbances $A(t)/A(21\ h)$ versus time during thermal treatment in the dark at 298 K of a 55 mM PA solution previously photolyzed for 4.5 h. $\lambda = 254$ (●, brown), 280 (●, yellow), 350 (●, green), 420 (●, purple), 450 (●, yellow/red), 700 (●, blue) nm. (B) Absorbance versus time during thermal treatment in the dark at 333 K of a 55 mM PA solution previously photolyzed for 4.5 h. At 20 h, the solution was diluted 1:2 with MQ water. λ(nm) = 264 (blue line), 254 (red line), 275 (green line).
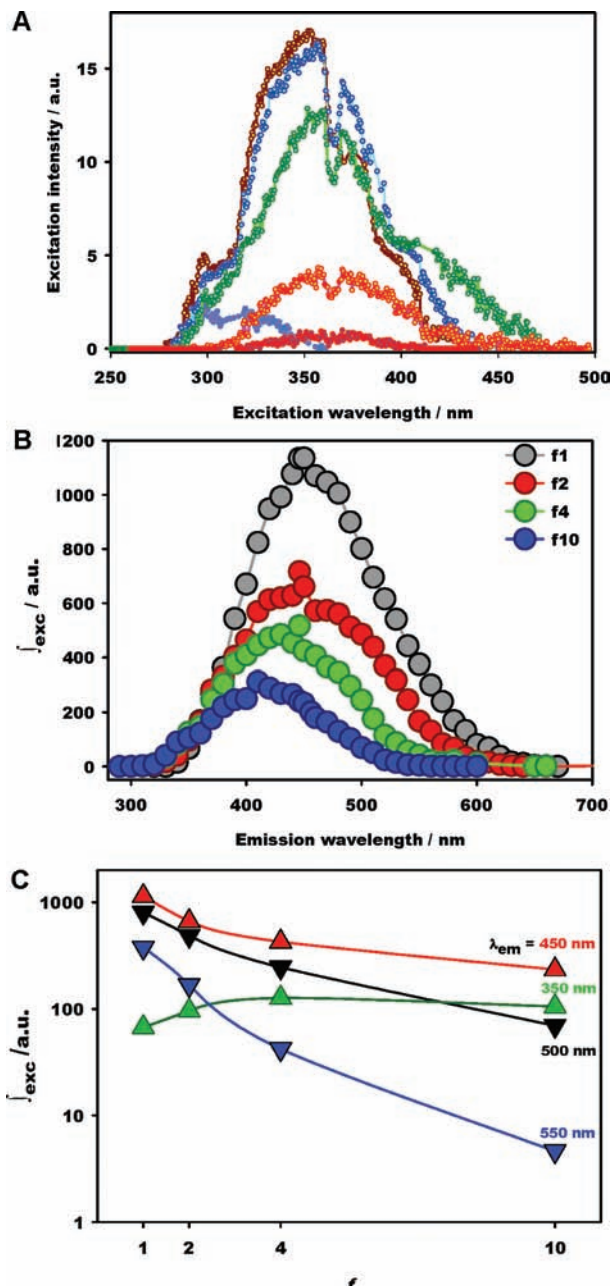
envelope.[36] The areas under fluorescence emission curves $\int_{em}$ (which are roughly proportional to fluorescence quantum yields Φ_f) peak at $\lambda_{exc} \approx 350$ nm (Figure 3B), whereas emission maxima wavelengths $^M\lambda_{em}$ increase linearly with λ_{exc} (inset to Figure 3B). Figure 3C shows how $\int_{em}(\lambda_{exc})$ values evolve by mere dilution with water. Notice that if our solutions contained independent fluorophores, $\int_{em}$ should decrease linearly with f at all λ_{exc} (dashed line in Figure 3C). Instead, $\int_{em}$ values decrease monotonically with f for $\lambda_{exc} \gtrsim 300$ nm (albeit not as expected), but emissions induced at shorter λ_{exc} are dramatically enhanced by several orders of magnitude. These opposing dependences on f are strong evidence that the fluorophores excited at $\lambda_{exc} \lesssim 300$ nm are intermolecularly coupled and partially transfer their excitation to acceptors emitting at longer wavelengths. Inner-filter effects could not fully account for these spectral effects or their magnitude.

Figure 4A shows corrected fluorescence excitation spectra of these solutions, which represent the absorption spectra of the species emitting at λ_{em}. Note that the most intense emissions are induced at $\lambda_{exc} \approx 350$ nm (Figure 3B), peak at $\lambda_{em} \approx 430$ nm (Figures 3A and Figure S2 in the Supporting Information), and comply with the reciprocity condition that the absorption spectrum of the species emitting at $\lambda_{em} \approx 430$ nm peaks at $\lambda_{exc} \approx 350$ nm (Figure 4A). Because absorption maxima for all λ_{em}
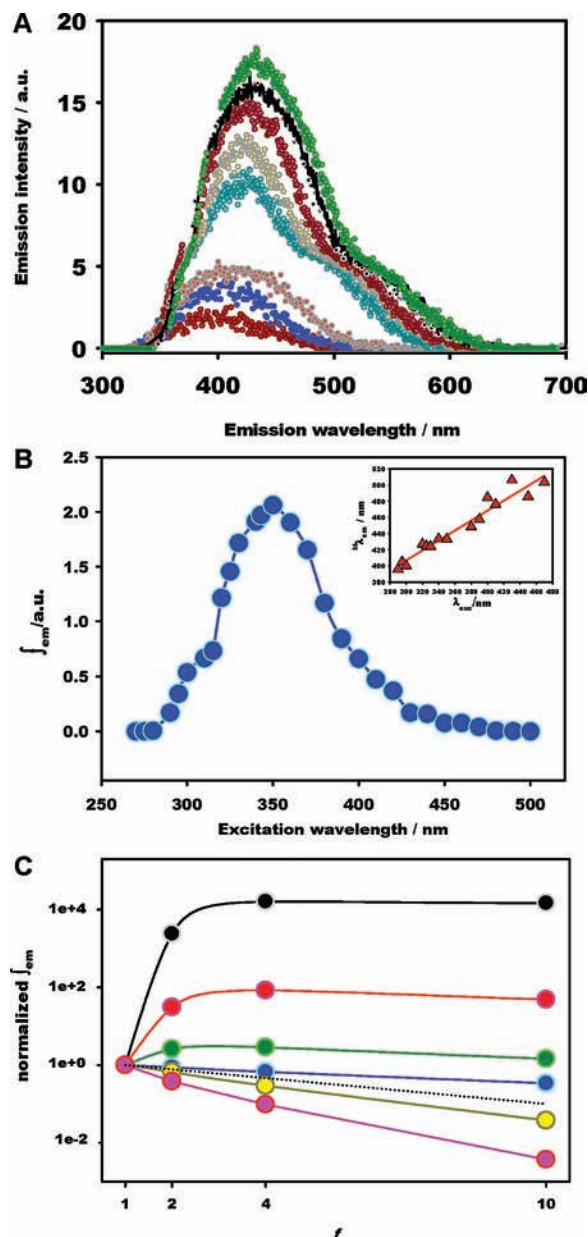
Figure 3. (A) Fluorescence emission spectra of 80 mM PA solution photolyzed for 4.5 h, followed by thermal treatment in the dark for 3 days at 333 K. $\lambda_{exc} = 290$ (●, red), 295 (●, dark blue), 300 (●, orange/gray), 320 (●, light blue), 325 (●, yellow/gray), 330 (●, pink), 340 (●, black), 350 (●, green) nm. (B) Areas under the emission curves of part A, $\int_{em}$ versus excitation wavelength λ_{exc}, for an 80 mM PA solution photolyzed for 4.5 h, followed by thermal treatment in the dark for 3 days at 333 K. The insert shows the position of emission maxima: $^M\lambda_{em}$ versus λ_{exc}. (C) Areas under emission curves $\int_{em}$ versus dilution factor f [areas normalized to $\int_{em}(f = 1) = 1$] for an 80 mM PA solution photolyzed for 4.5 h, followed by thermal treatment in the dark for 3 days at 333 K. $\lambda_{exc} = 270$ (●, black), 280 nm (●, red), 290 nm (●, green), 315 nm (●, blue), 400 nm (●, yellow), 460 nm (●, pink). The ideal inverse linear dependence of $\int_{em}$ on the dilution factor f is shown as the dotted curve.

occur at $\lambda_{exc} < 360$ nm (Figure 4A), excitations in the near-UV are transferred with variable efficiencies to a quasi-continuum of states emitting at longer wavelengths (up to $\lambda_{em} \approx 650$ nm). Figure 4B summarizes this information by showing the areas under the excitation (absorption) curves of Figure 4A, $\int_{exc}$, as a function of λ_{em} at various dilutions. Figure 4C shows the dependence of $\int_{exc}$ as a function of dilution at various λ_{em}. It is apparent that $\int_{exc}$ generally decreases with increasing dilution

Optical Absorptivity versus Molecular Composition

J. Phys. Chem. A, Vol. 113, No. 39, 2009 **10515**

Figure 4. (A) Excitation spectra of an 80 mM PA solution photolyzed for 4.5 h, followed by thermal treatment in the dark for 3 days at 333 K. Emission wavelengths λ_{em} = 350 (●, pink/blue), 430 (●, yellow/red), 450 (●, light blue), 480 (●, green), 560 (●, yellow/red), 620 (●, dark blue/red) nm. (B) Areas under the excitation curves of part A, $\int_{exc}$ versus λ_{em}, for an 80 mM PA solution photolyzed for 4.5 h, followed by thermal treatment in the dark for 3 days at 333 K at various dilution factors f. (C) Areas under excitation curves $\int_{exc}$ versus dilution factors f at various λ_{em} for a 80 mM PA solution photolyzed for 4.5 h, followed by thermal treatment in the dark for 3 days at 333 K. Emission wavelengths λ_{em}: 350 (▲, green), 450 (▲, red), 500 (▼, black) and 550 (▼, blue) nm.

for λ_{em} > 350 nm but increases for shorter wavelength emissions. The supramolecular aggregates underlying these phenomena apparently disassemble by mere dilution into smaller entities emitting at shorter wavelengths.

Figure 5A shows how PA and TOC decrease in the initial photolysis stage. The difference between the two curves represents the net amount of PA converted into organic species that remain in solution. Figure 5B shows TOC measurements
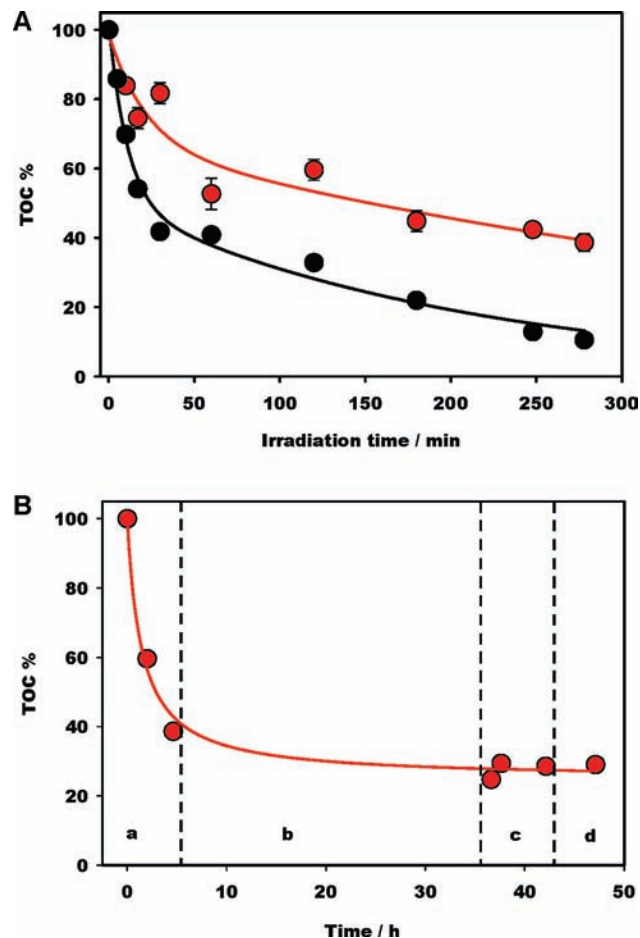

Figure 5. (A) Total organic carbon TOC% versus time during the photolysis of a 55 mM PA solution from TOC analysis (●, red) and calculated from PA losses (●, black). (B) Total organic carbon TOC%: (a) during photolysis of a 55 mM PA solution; (b) thermal treatment in the dark at 298 K; (c) rephotolysis; and (d) thermal treatment at 298 K.

along the various treatments. It is apparent that the largest carbon losses occur in the initial photolysis stage[92] and that subsequent photolytic and thermal treatments induce reversible transformations among species in solution that are not accompanied by further CO_2 releases.

Figure 6 shows ESI-MS of solutions after various stages (Scheme S1 in the Supporting Information). Note that the mass spectrum of the photolyzed solution (Figure 6A), whose absorption spectrum does not extend above $\lambda \approx 350$ (Figure 1A), is similar to that of the yellow solution produced after thermal treatment at 333 K for 3 days (Figure 6B) and also of the colorless solution obtained after rephotolysis for 1 h (Figure 6C). Further photolysis for 4.5 h, however, induces noticeable changes in the mass spectra (Figures 6D), but the mass spectrum of the yellow solution obtained by thermal treatment for 5.5 h is now very similar to that recorded immediately after prolonged photolysis (Figure 6E). These findings strikingly demonstrate that optical absorption spectra (color) are not correlated, in general, with the chemical compositions provided by ESI-MS of the corresponding solutions. Similar mass spectra are associated with colorless or yellow/brownish solutions, whereas solutions of different molecular compositions can be similarly tinted.

We also investigated whether high-molecular-weight products were generated in more dilute PA solutions. Figure 7A shows
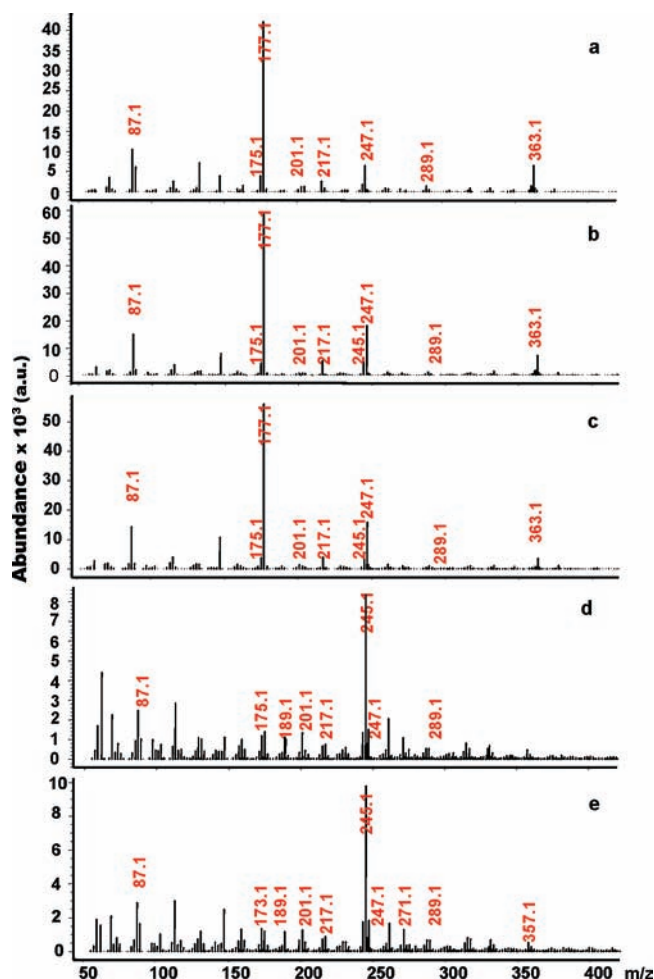
Figure 6. Electrospray ionization negative ion mass spectra. (a): 55 mM PA photolyzed for 4.5 h; (b): part a, followed by thermal treatment during 3 days dark at 333 K; (c): part b, followed by photolysis for 1 h; (d): part c, followed by photolysis for 4.5 h; and (e): part d after thermal treatment at 333 K for 5.5 h.

Figure 7. (A) Total ion abundance and average ion mass in electrospray ionization negative ion mass spectra versus initial pyruvic acid concentrations $[PA]_0$ after 4.5 h of photolysis. (B) Total ion abundance and average ion mass in electrospray ionization negative ion mass spectra after successive treatments. (I) 55 mM PA solution; (II) I after 4.5 photolysis 4.5 h; (III) II after thermal treatment at 333 K for 3 days; (IV) III after 1 h photolysis; (V) IV after thermal treatment at 333 K for 5.5 h.

how the sum of negative ion mass spectral signal intensities, or total ion abundance, ΣI_i, and average mass, $\langle M \rangle$,
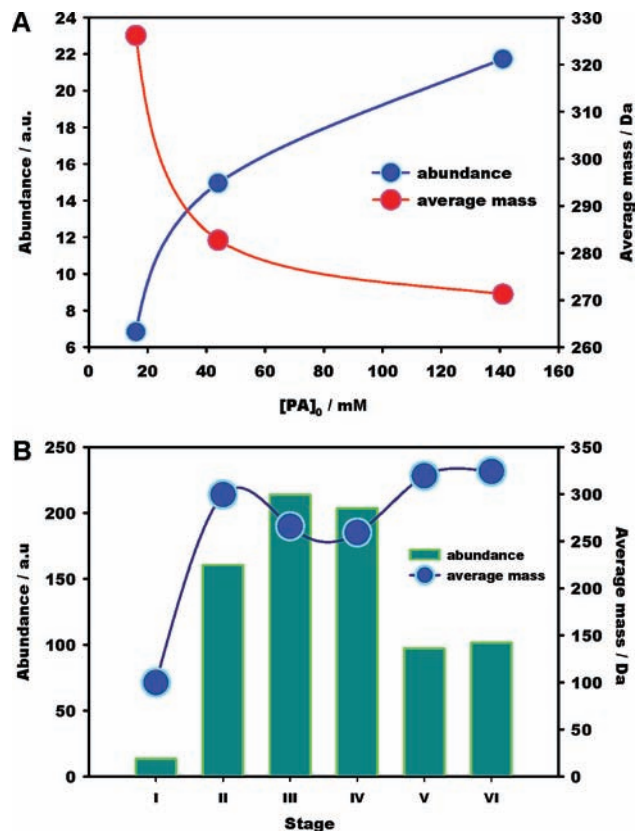
$$\text{total ion abundance} = \sum_{50}^{1500} I_i \quad (1)$$

$$\text{average mass} = \langle M \rangle = \frac{\sum_{50}^{1500} m_i I_i}{\sum_{50}^{1500} I_i} \quad (2)$$

vary with PA initial concentration $[PA]_0$. Interestingly, whereas ΣI_i decreases, as expected, $\langle M \rangle$ increases at lower $[PA]_0$, indicating the fact that higher mass products are produced from polymerization of simpler oligomers, rather than from PA itself, in PA-deficient solutions. Figure 7B shows how both parameters change in the various stages.

Discussion

General Considerations. Pyruvic acid, and other α-dicarbonyls that absorb solar $\lambda > 300$ nm radiation, are ubiquitous components of surface waters and the atmospheric aerosol.[83,93]

We chose PA as a surrogate for the light-absorbing species of the soluble OM present in atmospheric APs. The photolysis of PA at the micromolar concentrations prevalent in surface waters proceeds via unimolecular homolysis.[94] A transition from a unimolecular to a bimolecular process, however, is expected to occur above ~10 mM PA, that is, under conditions where the triplet excited state ${}^3PA^*$ becomes reactively quenched by PA itself ($k_Q \approx 2 \times 10^8$ M^{-1} s^{-1}) at rates competitive with its spontaneous decay ($k_{decay} = 2 \times 10^6$ s^{-1}) (Scheme 1A).[85,95,96] It should be realized that typical PA concentrations in atmospheric aerosols vastly exceed those in surface waters, and even more so should PA stand for the all α-dicarbonyls present, such as glyoxal and glyoxilic acid. For example, Kawamura et al. report $[PA]/[SO_4^{2-}] > 1 \times 10^{-3}$ molar ratios in urban aerosols.[83,97,98] Assuming that the upper limit to the water content of aerosol droplets is determined by the deliquescence curve of ammonium bisulfate solutions,[99–102] under 50% RH, aerosol should consist of droplets containing 0.6 g of H_2O/g of SO_4^{2-} or >20 mM PA under highly acidic conditions.[103]

Mechanism of Polymerization. We have previously shown that the $\lambda \geq 305$ nm photolysis of PA solutions yields a suite of polyfunctional oligomers via the radical polymerization mechanism shown in Scheme 1A,B.[85] The initiation involves photoinduced electron transfer between ${}^3PA^*$ and ground-state PA to produce a bound radical-ion pair.[95,104] The polymerization process is propagated by the addition of the isomeric radicals X• and Y• to PA and oligomer products, even in the presence of air because oxyl radicals Y• are not scavenged by O_2.[105] The

Optical Absorptivity versus Molecular Composition

J. Phys. Chem. A, Vol. 113, No. 39, 2009 **10517**

SCHEME 1: (A) Initial Processes during Photolysis of PA Solutions above ~10 mM (X•, Y•, and Z• Represent Ketyl, Alkoxyl, and Acetyl Radicals) and (B) Mechanism of the Photochemical Free Radical Oligomerization of Aqueous PA Solutions
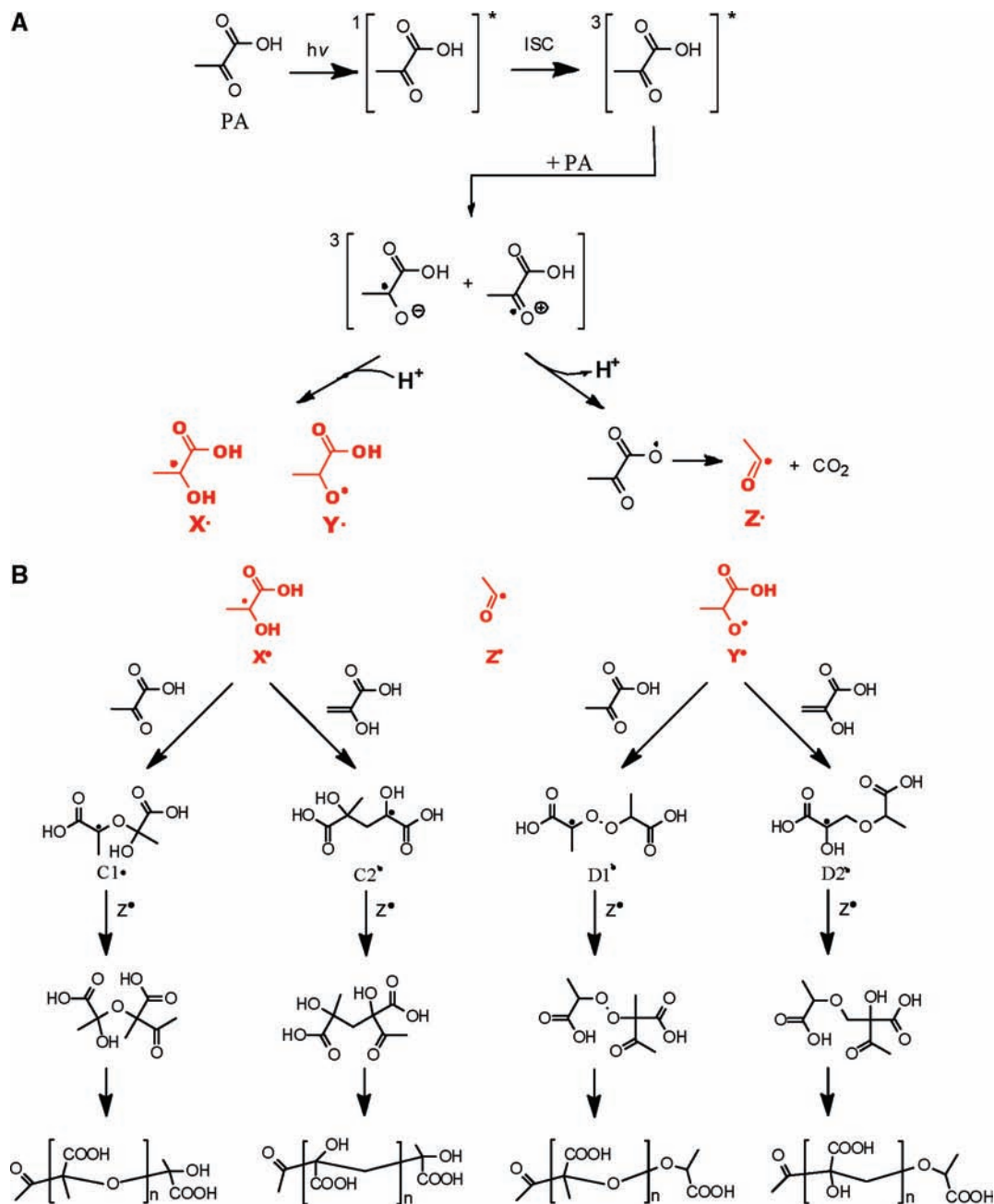
major TOC loss of the entire process (Figure 5B (a)) is associated with the fast decarboxylation of the primary acyloxyl radical $CH_3C(O)C(O)O•$ into the acetyl radical Z•, whose role as a terminating species incorporates a carbonyl chromophore into all oligomers. The prominent peak at $m/z = 177$ in Figure 6A−C may correspond to the anion of the 178 Da neutral species resulting from the recombination of X• and Y• radicals.[85] According to this mechanism, the $m/z = 247$ signals in Figure 6A−C correspond to anions of neutral species of mass 248 Da produced by recombination of C• and D• radicals (2 × 177 Da), followed by ($2CO_2 + H_2O$) losses (−106 Da) into $C_{10}H_{16}O_7$ species that are nearly isobaric with $C_9H_{12}O_8$. In principle, the molecular formulas of these species could be resolved by high-resolution mass spectrometry, and their structures could be identified by ^{1}H- and ^{13}C NMR analysis,[84] but the key point for present purposes is that they all consist of

aliphatic carboxylic acids containing ether, alcohol, and carbonyl functionalities arranged on flexible molecular backbones. Figure 7A shows that higher mass oligomers are produced in the photolysis of more dilute PA solutions. Figure 7B shows how total negative ion abundance (eq 1) and average mass (eq 2) vary along thermal and photochemical treatments. Note that average mass $\langle M \rangle$ reaches 300 Da after the first thermal treatment and fluctuates between 250 and 330 Da throughout.

Light Absorptivity. Color development in this and related systems arises from enhanced electronic coupling among the carbonyl chromophores embedded in polyfunctional oligomers. In our case, ultraviolet and visible absorptions are due to ($n \rightarrow \pi$) C=O transitions localized or electronically coupled to other carbonyls or to the C=C moieties resulting from intramolecular dehydration of neighboring alcohol groups.[74,106] Because the reversible color changes observed in our experiments upon

photolysis/thermal cycles are not accompanied by TOC losses, covalent bonding changes should involve isomerization or condensation reactions such as activated alcohol dehydrations or intra- or intermolecular esterifications during the dark periods[71] and their reverse processes upon photobleaching. Couplings among chromophores may be intramolecular, via electron delocalization through covalent or hydrogen bonds,[75,107] or through space, intra- or intermolecularly,[81,108] or via excimer/ exciplex formation.[82,109] Molecular self-assembly through non-covalent interactions is a common phenomenon among polar polyfunctional molecules, such as those generated photochemically in this system.[53,110–113] van der Waals forces and, in particular, hydrogen bonding can hold together chromophores brought closer within supramolecular aggregates via translational and rotational diffusion or backbone folding.[48,56,61,75]

Thermal Kinetics. The results of Figure 2A on the kinetics of color development at different wavelengths during prolonged thermal treatment of photolyzed solutions provide incisive clues about the nature of the transformations involved. Note that (1) because all species absorb at short wavelengths, but only some extend their absorptions into the visible, absorptions at specific wavelengths cannot be obviously associated with particular species, (2) most absorptions, except those at $\lambda \gtrsim 650$ nm, increase with nonzero initial slopes, as expected from first generation species, (3) only the shortest wavelength absorptions increase as single exponential growth functions, $A_\lambda(t) = A_\lambda(\infty) [1 - \exp(-k_\lambda t)]$, $\lambda \lesssim 270$ nm, whereas the rest evolve with stretched, or Kohlrausch kinetics, $A_\lambda(t) = A_\lambda(\infty) [1 - \exp(-k_\lambda t^n)]$, $n < 1$,[89,114,115] and (4) rates increase markedly with temperature; that is, some of the processes involved in color development have sizable activation energies associated with the breaking and forming of covalent bonds. These observations indicate that the oligomers produced by photolysis already provide building blocks for aggregates. However, slow, thermally activated chemical reactions also produce new macromolecular species that participate in the later stages of the aggregation process. These new macromolecular species can be subsequently bleached but cannot be destroyed by simple dilution (Figure 1A,B). The range of electron delocalization among chromophores is thereby extended, and the long wavelength tails of the spectra are shifted to the red. The moieties absorbing above $\lambda \approx 650$ nm have vanishing initial slopes, indicating that their production requires and is consecutive to the generation of novel precursors. The intriguing small amplitude absorbance oscillations of period $\tau = 4.2$ h observed in Figure 2B under anoxic conditions may signal the reversible thermal keto–enol isomerizations likely taking place in our system.[116,117]

Fluorescence Emissions. Fluorescence emissions from these solutions display even more dramatic evidence of supramolecular interactions. Whereas the initial or photolyzed PA solutions display minimal fluorescence (Figure S1 in the Supporting Information), their thermal treatment yields solutions that fluoresce strongly in the near UV and visible regions up to $\lambda_{em} \approx 700$ nm (Figure 3A and Figure S2 in the Supporting Information). With few exceptions, fluorescence from a single chromophore in condensed phase originates from the lowest excited state, leading to emission spectra and fluorescence quantum yields that are independent of excitation wavelength, λ_{exc}.[109] Figure 3A,B shows that none of these outcomes is realized in this system, pointing to strongly interacting chromophores/fluorophores. Interactions may involve ground states

SCHEME 2: One of the Possible Structures of the Supramolecular Dimer of the 308 Da ($C_{11}H_{16}O_{10}$) Oligomer ($n = 2$ in Scheme 1B) Produced in the Photolysis of PA Solutions As Held Together by Intermolecular Hydrogen Bonds[a]
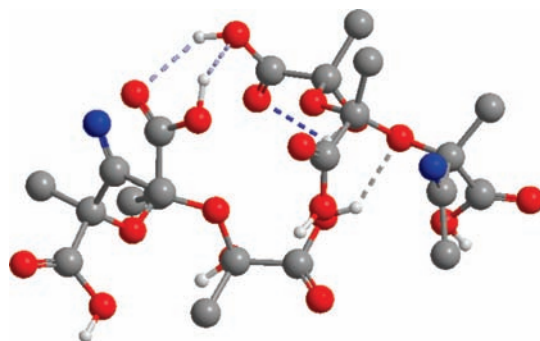
[a] Blue O atoms correspond to carbonyl groups.

to account for red-shifted absorption spectra and also excited states, given the linear increase of $^M\lambda_{em}$ with λ_{exc} (inset, Figure 3B).

A significant observation is that emission spectra excited at $\lambda_{exc} \gtrsim 400$ nm are enveloped by the spectrum generated by $\lambda_{exc} = 350$ nm (Figure 3A and Figure S2 in the Supporting Information), that is, that the fluorophores excited at longer wavelengths are a lower energy subset of those populated by $\lambda_{exc} = 350$ nm. This behavior evokes the fluorescence properties of natural fulvic acids reported by Del Vecchio and Blough[36] and can be rationalized by a scheme in which the initial excitation is transferred to a dense manifold of emitting states. Our system, however, differs from fulvic acids in two important aspects because: (1) emissions become less intense at $\lambda_{exc} \leq 350$ nm and (2) the dramatic dilution effects shown in Figure 3C represent definitive evidence of intermolecular rather than intramolecular couplings/energy transfer.[109] The opposite dependences of the areas under excitation curves, that is, the total radiation absorbed that is reemitted at λ_{em} (Figure 4B), to dilution above and below $\lambda_{em} \approx 400$ nm (Figure 4C), are also consistent with absorptions and emissions from supramolecular aggregates that can be disrupted by mere dilution.

In summary, the kinetics of color development in the dark (Figure 2A,B) and dilution effects on absorption (Figures 1B and 4C) and fluorescence spectra (Figure 3C) provide direct evidence of: (1) typical polar, polyfunctional macromolecules of moderate complexity aggregate spontaneously, (2) isolated chromophores-in-macromolecules become electronically coupled in these aggregates, thereby absorbing more intensely and at longer wavelengths; that is, visible absorptions may be generated in the dark from colorless species,[37] and (3) long-wavelength absorptions can be instantly removed by mere dilution, and protractedly by photobleaching. Below we analyze the potential implications of these results on the optical properties of the organic aerosol and whether some of these phenomena have been actually observed in the field.

Environmental Implications. In the fourth assessment report of the Intergovernmental Panel on Climate Change (IPCC), the effect on climate of APs was estimated to be $\sim 20\%$ of that of greenhouse gases.[2] Aerosols are generally considered to have a cooling effect, which would partially mitigate global warming, because they mainly scatter incoming solar radiation by increasing the albedo at the top of the atmosphere (TOA). Actual effects are far more complex, and comprise direct effects via radiation scattering and absorption, indirect effects via cloud nucleation,

Optical Absorptivity versus Molecular Composition

J. Phys. Chem. A, Vol. 113, No. 39, 2009 **10519**

and semidirect effects on atmospheric temperature profiles, moisture fluxes, and convection.[7,18] Recent models emphasize the sensitivity of cloud properties and the persistence of mountain glaciers to the aerosol single-scattering albedo: SSA = $\sigma_S/(\sigma_S + \sigma_A)$ (σ_S and σ_A are the aerosol scattering and absorption coefficients).[18] The semidirect effects introduce additional feedback mainly through σ_A. The warming of the atmosphere above 2 km altitude due to absorption of visible radiation by the aerosol tends to inhibit cloudiness and cause the irreversible melting of the snowcaps that supply the major rivers that sustain agriculture in the most populated regions of the world.[7]

The SSA dependences on wavelength and RH are the key factors that determine the radiative effects of the aerosol. Hygroscopic APs swell at higher RH, thereby increasing σ_S.[65] State-of-the art models evaluate the absorptivity of the aerosol by assuming linear additivity of volume-weighted absorptivities of internally mixed components.[18] In other words, σ_A is assumed to be a linearly decreasing function of the water content of the aerosol. Our results clearly suggest otherwise. At low RH, the aerosol may absorb more visible radiation than expected from this simple assumption, thereby providing an extra positive feedback to semidirect effects on cloud dissipation.

There is evidence of daily (dark and light) cycles for σ_S and σ_A of the aerosol over Mexico City under conditions where total carbon concentrations in <1 μm aerosol samples remained relatively constant at (15 ± 5) μg m^{-3} during measurements (from March 10 to March 29).[33] Absorption represented a substantial fraction of the aerosol refractive index, with SSA values ranging from 0.35 to 0.90. σ_A values peak early in the morning (at ~6:00 local time) and reach minima after noon (~13:00 local time), that is, under conditions of maximum photochemical processing, whereas σ_S values peak ~4 h later. We interpret these observations as confirmation that σ_A increases at nighttime because of dark reactions in the aerosol phase and decreases because of photobleaching under insolation. Particle size, which reflects aerosol production and largely affects σ_S, has a different daily cycle.

Conclusions

Our study highlights the key role that condensed-phase organic photochemistry plays in aerosol science. It also shows that solutions of polar, polyfunctional, chromophoric oligomers, such as those found in natural HULIS, aggregate into supramolecular complexes that display red-shifted absorption and fluorescence spectra. Supramolecular complexes absorb and emit more intensely and over a wider spectral range than a system of noninteracting oligomer blocks. The optical absorptivity of supramolecular aggregates depends nonlinearly on dilution and can be readily photobleached. These phenomena are deemed to be particularly relevant to the modeling of the optical properties of atmospheric aerosols.

Supporting Information Available: Additional data, data analysis, and experimental details. This material is available free of charge via the Internet at http://pubs.acs.org.

Note Added after ASAP Publication. This article posted ASAP on August 28, 2009. Figure 4C has been revised. The corrected version posted on September 3, 2009.

References and Notes

(1) Houghton, J. T.; Ding, Y.; Griggs, D. J.; Noguer, M.; van der Linden, P.; Dai, X.; Maskell, K.; Johnston, C. A. *Climate Change 2001: The Scientific Basis*; Cambridge University Press: Cambridge, U.K., 2001.

(2) Forster, P., et al. *Climate Change 2007: The Physical Science Basis: Fourth Assessment Report of the Intergovernmental Panel on Climate Change*; 2007. http://www.ipcc.ch/.

(3) Charlson, R. J.; Schwartz, S. E.; Hales, J. M.; Cess, R. D.; Coakley, J. A.; Hansen, J. E.; Hofmann, D. J. *Science* **1992**, *255*, 423.

(4) Kanakidou, M.; Seinfeld, J. H.; Pandis, S. N.; Barnes, I.; Dentener, F. J.; Facchini, M. C.; Van Dingenen, R.; Ervens, B.; Nenes, A.; Nielsen, C. J.; Swietlicki, E.; Putaud, J. P.; Balkanski, Y.; Fuzzi, S.; Horth, J.; Moortgat, G. K.; Winterhalter, R.; Myhre, C. E. L.; Tsigaridis, K.; Vignati, E.; Stephanou, E. G.; Wilson, J. *Atmos. Chem. Phys.* **2005**, *5*, 1053.

(5) Hoyle, C. R.; Berntsen, T.; Myhre, G.; Isaksen, I. S. A. *Atmos. Chem. Phys.* **2007**, *7*, 5675.

(6) Ramanathan, V.; Crutzen, P. J. *Atmos. Environ.* **2003**, *37*, 4033.

(7) Ramanathan, V.; Ramana, M. V.; Roberts, G.; Kim, D.; Corrigan, C.; Chung, C.; Winker, D. *Nature* **2007**, *448*, 575.

(8) Zhang, H.; Wang, Z. L.; Guo, P. W.; Wang, Z. Z. *Adv. Atmos. Sci.* **2009**, *26*, 57.

(9) Pöschl, U. *Angew. Chem., Int. Ed.* **2005**, *44*, 7520.

(10) Stier, P.; Seinfeld, J. H.; Kinne, S.; Boucher, O. *Atmos. Chem. Phys.* **2007**, *7*, 5237.

(11) Menon, S.; Hansen, J.; Nazarenko, L.; Luo, Y. F. *Science* **2002**, *297*, 2250.

(12) Kokkola, H.; Sorjamaa, R.; Peraniemi, A.; Raatikainen, T.; Laaksonen, A. *Geophys. Res. Lett.* **2006**, *33*, L10816.

(13) Dinar, E.; Riziq, A. A.; Spindler, C.; Erlick, C.; Kiss, G.; Rudich, Y. *Faraday Discuss.* **2008**, *137*, 279.

(14) Rosenfeld, D.; Lohmann, U.; Raga, G. B.; O'Dowd, C. D.; Kulmala, M.; Fuzzi, S.; Reissell, A.; Andreae, M. O. *Science* **2008**, *321*, 1309.

(15) Dinar, E.; Taraniuk, I.; Graber, E. R.; Katsman, S.; Moise, T.; Anttila, T.; Mentel, T. F.; Rudich, Y. *Atmos. Chem. Phys.* **2006**, *6*, 2465.

(16) Ghan, S. J.; Schwartz, S. E. *Bull. Amer. Meteorol. Soc.* **2007**, *88*, 1059.

(17) Facchini, M. C.; Fuzzi, S.; Zappoli, S.; Andracchio, A.; Gelencser, A.; Kiss, G.; Krivacsy, Z.; Meszaros, E.; Hansson, H. C.; Alsberg, T.; Zebuhr, Y. *J. Geophys. Res.* **1999**, *104*, 26821.

(18) Fan, J. W.; Zhang, R. Y.; Tao, W. K.; Mohr, K. I. *J. Geophys. Res.* **2008**, *113*, D08209.

(19) Koch, D.; Bond, T. C.; Streets, D.; Unger, N. *Geophys. Res. Lett.* **2007**, *34*, L05821.

(20) Koch, D.; Bond, T. C.; Streets, D.; Unger, N.; van der Werf, G. R. *J. Geophys. Res.* **2007**, *112*, D02205.

(21) Roger, J. C.; Mallet, M.; Dubuisson, P.; Cachier, H.; Vermote, E.; Dubovik, O.; Despiau, S. *J. Geophys. Res.* **2006**, *111*, D13208.

(22) Unger, N.; Shindell, D. T.; Koch, D. M.; Streets, D. G. *J. Geophys. Res.* **2008**, *113*, D02306.

(23) Rudich, Y.; Donahue, N. M.; Mentel, T. F. *Annu. Rev. Phys. Chem.* **2007**, *58*, 321.

(24) Gelencser, A.; Hoffer, A.; Krivacsy, Z.; Kiss, G.; Molnar, A.; Meszaros, E. *J. Geophys. Res.* **2002**, *107*, D4137.

(25) Feng, J. S.; Moller, D. *J. Atmos. Chem.* **2004**, *48*, 217.

(26) Kiss, G.; Varga, B.; Gelencser, A.; Krivacsy, Z.; Molnar, A.; Alsberg, T.; Persson, L.; Hansson, H. C.; Facchini, M. C. *Atmos. Environ.* **2001**, *35*, 2193.

(27) Kiss, G.; Varga, B.; Galambos, I.; Ganszky, I. *J. Geophys. Res.* **2002**, *107*, 8339.

(28) Hoffer, A.; Gelencser, A.; Blazso, M.; Guyon, P.; Artaxo, P.; Andreae, M. O. *Atmos. Chem. Phys.* **2006**, *6*, 3505.

(29) Hoffer, A.; Gelencser, A.; Guyon, P.; Kiss, G.; Schmid, O.; Frank, G. P.; Artaxo, P.; Andreae, M. O. *Atmos. Chem. Phys.* **2006**, *6*, 3563.

(30) Bergstrom, R. W.; Pilewskie, P.; Russell, P. B.; Redemann, J.; Bond, T. C.; Quinn, P. K.; Sierau, B. *Atmos. Chem. Phys.* **2007**, *7*, 5937.

(31) Bates, T. S.; Anderson, T. L.; Baynard, T.; Bond, T.; Boucher, O.; Carmichael, G.; Clarke, A.; Erlick, C.; Guo, H.; Horowitz, L.; Howell, S.; Kulkarni, S.; Maring, H.; McComiskey, A.; Middlebrook, A.; Noone, K.; O'Dowd, C. D.; Ogren, J.; Penner, J.; Quinn, P. K.; Ravishankara, A. R.; Savoie, D. L.; Schwartz, S. E.; Shinozuka, Y.; Tang, Y.; Weber, R. J.; Wu, Y. *Atmos. Chem. Phys.* **2006**, *6*, 1657.

(32) Barnard, J. C.; Volkamer, R.; Kassianov, E. I. *Atmos. Chem. Phys.* **2008**, *8*, 6665.

(33) Marley, N. A.; Gaffney, J. S.; Castro, T.; Salcido, A.; Frederick, J. *Atmos. Chem. Phys.* **2009**, *9*, 189.

(34) Rodwell, M. J.; Jung, T. Q. J. R. *Meteorol. Soc.* **2008**, *134*, 1479.

(35) Bao, Z. H.; Wen, Z. P.; Wu, R. G. *J. Geophys. Res., [Atmos.]* **2009**, *114*, D05203.

(36) Del Vecchio, R.; Blough, N. V. *Environ. Sci. Technol.* **2004**, *38*, 3885.

(37) Sun, H. L.; Biedermann, L.; Bond, T. C. *Geophys. Res. Lett.* **2007**, *34*, L17813.

(38) Havers, N.; Burba, P.; Lambert, J.; Klockow, D. *J. Atmos. Chem.* **1998**, *29*, 45.

(39) Goldstein, A. H.; Galbally, I. E. *Environ. Sci. Technol.* **2007**, *41*, 1514.

(40) Graber, E. R.; Rudich, Y. *Atmos. Chem. Phys.* **2006**, *6*, 729.

(41) Kalberer, M. *Anal. Bioanal. Chem.* **2006**, *385*, 22.

(42) Kroll, J. H.; Seinfeld, J. H. *Atmos. Environm.* **2008**, *42*, 3593.

(43) Samburova, V.; Didenko, T.; Kunenkov, E.; Emmenegger, C.; Zenobi, R.; Kalberer, M. *Atmos. Environm.* **2007**, *41*, 4703.

(44) Samburova, V.; Szidat, S.; Hueglin, C.; Fisseha, R.; Baltensperger, U.; Zenobi, R.; Kalberer, M. *J. Geophys. Res.* **2005**, *110*, D23210.

(45) Samburova, V.; Zenobi, R.; Kalberer, M. *Atmos. Chem. Phys.* **2005**, *5*, 2163.

(46) Kalberer, M.; Paulsen, D.; Sax, M.; Steinbacher, M.; Dommen, J.; Prevot, A. S. H.; Fisseha, R.; Weingartner, E.; Frankevich, V.; Zenobi, R.; Baltensperger, U. *Science* **2004**, *303*, 1659.

(47) Kalberer, M.; Sax, M.; Samburova, V. *Environ. Sci. Technol.* **2006**, *40*, 5917.

(48) MacCarthy, P. *Soil Sci.* **2001**, *166*, 738.

(49) Hertkorn, N.; Frommberger, M.; Witt, M.; Koch, B. P.; Schmitt-Kopplin, P.; Perdue, E. M. *Anal. Chem.* **2008**, *80*, 8908.

(50) Hertkorn, N.; Ruecker, C.; Meringer, M.; Gugisch, R.; Frommberger, M.; Perdue, E. M.; Witt, M.; Schmitt-Kopplin, P. *Anal. Bioanal. Chem* **2007**, *389*, 1311.

(51) Koch, B. P.; Ludwichowski, K. U.; Kattner, G.; Dittmar, T.; Witt, M. *Mar. Chem.* **2008**, *111*, 233.

(52) Schmitt-Kopplin, P.; Hertkorn, N. *Anal. Bioanal. Chem.* **2007**, *389*, 1309.

(53) Sutton, R.; Sposito, G. *Environ. Sci. Technol.* **2005**, *39*, 9009.

(54) Peuravuori, J.; Bursakova, P.; Pihlaja, K. *Anal. Bioanal. Chem.* **2007**, *389*, 1559.

(55) Peuravuori, J. *Environ. Sci. Technol.* **2005**, *39*, 5541.

(56) Yagai, S. *J. Photochem. Photobiol., C* **2006**, *7*, 164.

(57) Peuravuori, J.; Pihlaja, K. *Environ. Sci. Technol.* **2004**, *38*, 5958.

(58) Pluth, M. D.; Raymond, K. N. *Chem. Soc. Rev.* **2007**, *36*, 161.

(59) Zhao, J.; Khalizov, A.; Zhang, R. Y.; McGraw, R. *J. Phys. Chem. A* **2009**, *113*, 680.

(60) Schwalb, N. K.; Temps, F. *Science* **2008**, *322*, 243.

(61) Schaumann, G. E.; Bertmer, M. *Eur. J. Soil Sci.* **2008**, *59*, 423.

(62) Langhals, H.; Abbt-Braun, G.; Frimmel, F. H. *Acta Hydrochim. Hydrobiol.* **2000**, *28*, 329.

(63) Duarte, R.; Pio, C. A.; Duarte, A. C. *Anal. Chim. Acta* **2005**, *530*, 7.

(64) Peuravuori, J.; Pihlaja, K. *Anal. Chim. Acta* **1997**, *337*, 133.

(65) Garland, R. M.; Ravishankara, A. R.; Lovejoy, E. R.; Tolbert, M. A.; Baynard, T. *J. Geophys. Res.* **2007**, *112*, D19303.

(66) McQuarrie, D. A. *Statistical Thermodynamics*; University Science Books: Mill Valley, CA, 1973.

(67) Aiken, A. C.; Decarlo, P. F.; Kroll, J. H.; Worsnop, D. R.; Huffman, J. A.; Docherty, K. S.; Ulbrich, I. M.; Mohr, C.; Kimmel, J. R.; Sueper, D.; Sun, Y.; Zhang, Q.; Trimborn, A.; Northway, M.; Ziemann, P. J.; Canagaratna, M. R.; Onasch, T. B.; Alfarra, M. R.; Prevot, A. S. H.; Dommen, J.; Duplissy, J.; Metzger, A.; Baltensperger, U.; Jimenez, J. L. *Environ. Sci. Technol.* **2008**, *42*, 4478.

(68) Reemtsma, T.; These, A.; Springer, A.; Linscheid, M. *Environ. Sci. Technol.* **2006**, *40*, 5839.

(69) Rudich, Y. *Chem. Rev.* **2003**, *103*, 5097.

(70) Noziere, B.; Esteve, W. *Atmos. Environ.* **2007**, *41*, 1150.

(71) Fiedler, T.; Kroh, L. W. *Eur. Food Res. Technol.* **2007**, *225*, 473.

(72) Reid, J. S.; Koppmann, R.; Eck, T. F.; Eleuterio, D. P. *Atmos. Chem. Phys.* **2005**, *5*, 799.

(73) Shapiro, E. L.; Szprengiel, J.; Sareen, N.; Jen, C. N.; Giordano, M. R.; McNeill, V. F. *Atmos. Chem. Phys.* **2009**, *9*, 2289.

(74) Yamaguchi, Y.; Matsubara, Y.; Ochi, T.; Wakamiya, T.; Yoshida, Z. I. *J. Am. Chem. Soc.* **2008**, *130*, 13867.

(75) Ward, M. D. *Chem. Soc. Rev.* **1997**, *26*, 365.

(76) Volkov, P. A.; Drozdov, A. Y.; Fadeev, V. V. *Laser Phys.* **2007**, *17*, 1271.

(77) Puchalski, M. M.; Morra, M. J.; Vonwandruszka, R. *Environ. Sci. Technol.* **1992**, *26*, 1787.

(78) Macdonald, R. I. *J. Biol. Chem.* **1990**, *265*, 13533.

(79) Kumke, M. U.; Abbt-Braun, G.; Frimmel, F. H. *Acta Hydrochim. Hydrobiol.* **1998**, *26*, 73.

(80) Keizer, J. *J. Am. Chem. Soc.* **1983**, *105*, 1494.

(81) Jiang, Z. J.; Goedel, W. A. *Phys. Chem. Chem. Phys.* **2008**, *10*, 4584.

(82) Jenekhe, S. A.; Osaheni, J. A. *Science* **1994**, *265*, 765.

(83) Ho, K. F.; Cao, J. J.; Lee, S. C.; Kawamura, K.; Zhang, R. J.; Chow, J. C.; Watson, J. G. *J. Geophys. Res.* **2007**, *112*, D22S27.

(84) Rincón, A. G.; Guzmán, M. I.; Hoffmann, M. R.; Colussi, A. J., in preparation.

(85) Guzmán, M. I.; Colussi, A. J.; Hoffmann, M. R. *J. Phys. Chem. A* **2006**, *110*, 3619.

(86) Gonsior, M.; Peake, B. M.; Cooper, W. T.; Podgorski, D.; D'Andrilli, J.; Cooper, W. J. *Environ. Sci. Technol.* **2009**, *43*, 698.

(87) Anastasio, C.; Robles, T. *J. Geophys. Res.* **2007**, *112*, D24304.

(88) Kieber, R. J.; Willey, J. D.; Whitehead, R. F.; Reid, S. N. *J. Atmos. Chem.* **2007**, *58*, 219.

(89) Sabelko, J.; Ervin, J.; Gruebele, M. *Proc. Natl. Acad. Sci. U.S.A.* **1999**, *96*, 6031.

(90) Quintas, M. A. C.; Brandao, T. R. S.; Silva, C. L. M. *J. Food Eng.* **2007**, *83*, 483.

(91) Pirrung, M. C.; Das Sarma, K. *J. Am. Chem. Soc.* **2004**, *126*, 444.

(92) Kieber, R. J.; Zhou, X.; Mopper, K. *Limnol. Oceanogr.* **1990**, *35*, 1503.

(93) Kawamura, K.; Yasui, O. *Atmos. Environ.* **2005**, *39*, 1945.

(94) Kieber, D. J.; Blough, N. V. *Free Radical Res. Commun.* **1990**, *10*, 109.

(95) Davidson, R. S.; Goodwin, D.; Fornier de Violet, P. *Chem. Phys. Lett.* **1981**, *78*, 471.

(96) Guzmán, M. I.; Colussi, A. J.; Hoffmann, M. R. *J. Phys. Chem. A* **2006**, *110*, 931.

(97) Kawamura, K.; Imai, Y.; Barrie, L. A. *Atmos. Environ.* **2005**, *39*, 599.

(98) Kawamura, K.; Watanabe, T. *Anal. Chem.* **2004**, *76*, 5762.

(99) Saxena, P.; Hildemann, L. M. *Environ. Sci. Technol.* **1997**, *31*, 3318.

(100) Kreidenweis, S. M.; Petters, M. D.; DeMott, P. J. *Environ. Res. Lett.* **2008**, 3.

(101) Petters, M. D.; Kreidenweis, S. M. *Atmos. Chem. Phys.* **2008**, *8*, 6273.

(102) Salma, I.; Ocskay, R.; Lang, G. G. *Atmos. Chem. Phys.* **2008**, *8*, 2243.

(103) Jang, M.; Czoschke, N. M.; Northcross, A. L. *Environ. Sci. Technol.* **2005**, *39*, 164.

(104) Davidson, R. S.; Goodwin, D. *J. Chem. Soc., Perkin Trans. 2* **1982**, 1559.

(105) Hartung, J.; Gottwald, T.; Spehar, K. *Synthesis* **2002**, 1469.

(106) Hsu, C. P. *Acc. Chem. Res.* **2009**, *42*, 509.

(107) Rubin, M. B.; Gleiter, R. *Chem. Rev.* **2000**, *100*, 1121.

(108) Majumdar, Z. K.; Hickerson, R.; Noller, H. F.; Clegg, R. M. *J. Mol. Biol.* **2005**, *354*, 504.

(109) Turro, N. J. *Modern Molecular Photochemistry*; University Science Books: Sausalito, CA, 1991.

(110) Tabazadeh, A. *Atmos. Environ.* **2005**, *39*, 5472.

(111) Baigorri, R.; Fuentes, M.; Gonzalez-Gaitano, G.; Garcia-Mina, J. M. *J. Phys. Chem. B* **2007**, *111*, 10577.

(112) Lehn, J. M. *Proc. Natl. Acad. Sci. U.S.A.* **2002**, *99*, 4763.

(113) Lehn, J. M. *Science* **2002**, *295*, 2400.

(114) Shlesinger, M. F.; Zaslavsky, G. M.; Klafter, J. *Nature* **1993**, *363*, 31.

(115) Volk, M.; Kholodenko, Y.; Lu, H. S. M.; Gooding, E. A.; DeGrado, W. F.; Hochstrasser, R. M. *J. Phys. Chem. B* **1997**, *101*, 8607.

(116) Sajewicz, M.; Gontarska, M.; Kronenbach, D.; Kowalska, T. *Acta Chromatogr.* **2008**, *20*, 209.

(117) Sajewicz, M.; Gontarska, M.; Wojtal, L.; Kronenbach, D.; Leda, M.; Epstein, I. R.; Kowalska, T. *J. Liq. Chromatogr. Relat. Technol.* **2008**, *31*, 1986.